

Overdrive Short Pulse High Peak Power Diode Lasers Without Catastrophic Optical Damage

Miguel Sánchez , Daniel Gallego, and Horacio Lamela

Abstract—Light Imaging Detection and Ranging (LIDAR) and Optoacoustic biomedical imaging techniques are applications that have a specific laser source requirements: short pulses, high peak power per pulse and high repetition rates. A custom current driver has been designed to fulfill these requirements and characterized in order to generate high current short pulses to drive High Power Diode Lasers (HPDL) beyond their maximum rating value, with a maximum current capacity of 120 A in a range of less than 10 nanoseconds pulse width, rise times up to 2 ns and a repetition rate of 1 kHz. Four commercial HPDLs have been driven generating optical pulses of less than 10 ns and more than four times the maximum rated optical peak power. A single laser device reached a maximum peak power of 880.6 W at 6 ns pulse width, demonstrating stable operation without catastrophic optical damage and improving the typical operation characteristics of the HPDLs for high speed short pulse applications.

Index Terms—Diode lasers, laser damage, ultrafast lasers, semiconductor lasers.

I. INTRODUCTION

NEW applications such as Light Imaging Detection and Ranging (LIDAR) for autonomous driving and optoacoustic biomedical imaging techniques require pulsed laser light sources with large peaks power and short pulse duration in the range of few nanoseconds.

LIDAR based on time of flight (TOF) is a procedure for determine distances to a target using pulsed laser light and an optical detector that measures the reflected light. Differences in the laser round trip time is used to make a geographically accurate three-dimensional (3D) point cloud of an environment. This technique is extensively used in many fields such as topography [1] speed detection [2], object detection [3], 3D maps [4] and for autonomous driver assistance systems [5]. Onboard LIDAR system applications require laser sources compact, reliable and easily integrated like High Power Diode Lasers (HPDLs). Currently, the pervasiveness of these 3D mapping sensors in the automotive industry makes that the mass production capability and the cost reduction in the overall system other relevant requirements. The three most decisive parameters of the pulsed laser source for this

application are the peak power that determines the measurement distance, the pulse width that limits the spatial resolution and the repetition rate that defines the image acquisition time.

Optoacoustic imaging techniques, which are also known as photoacoustic, such as Optoacoustic Tomography (OAT) [6], [7] and Optoacoustic Microscopy (OAM) [8], [9], are innovative biomedical imaging that combines the contrast and specificity of the optical imaging with the resolution of the ultrasound images. They are based on the optoacoustic effect, that describes the conversion of pulses of light absorbed by a sample into pressure waves. The broadband ultrasound waves generated by this effect can be used, as well, for enhanced ultrasound imaging in the so-called Laser Ultrasound (LUS) [10], [11]. These optoacoustic applications use laser sources able to: emit short pulses, less than one hundred nanoseconds, to generate broadband ultrasound waves for high-resolution imaging; energies between several μJ to few mJ, to reach 1 to 4 cm penetration depth; and high repetition rates (kHz) for obtaining real-time images [12].

Solid state lasers, such as Q-switched Nd-YAG lasers, can provide large amounts of energy (up to hundreds of millijoules when they are combined with an OPO) and short optical pulses with a fixed duration of few nanoseconds. Nonetheless, bearing in mind the laser head and its power supply, they are complex, ponderous, hardly portable, expensive, depends upon recurrent maintenance and have low repetition rates in the range of 10 to 100 Hz. Repetition rates can be expanded to tenths of kHz and the size can be decreased through the use of diode pumped solid state lasers [13] with a considerable reduction of energy.

Currently, advances in semiconductor laser device construction technologies are allowing the commercialization of diode laser devices with high powers and low prices. These HPDLs can reach output power of hundreds of watts, starting to be used in applications where the use of solid states lasers was exclusive, such as materials processing [14], gas detection [15] and multiple biomedical applications [16]. They are compact, robust and very cost-effective. Current drivers allow the control of the pulse peak power, the pulse width, that can vary in the range from few nanoseconds to few hundred nanoseconds, and the repetition rate up to several kilohertz. In particular, to generate short optical pulses and high peak powers with HPDLs, it is necessary the development of specific high-speed driver electronics and optimized designs that can bring very high current pulses (hundreds A to few kA) with fast rise times and short width pulses in the range of few nanoseconds. However, the energies reached by current HPDLs are not enough for short pulse applications showing lower performance compared

Manuscript received April 20, 2021; revised June 14, 2021; accepted June 24, 2021. Date of publication June 30, 2021; date of current version July 28, 2021. This work was supported by Comunidad de Madrid under Grant S2018/NMT-4333MARTINLARA-CM project within the Programa de Actividades de I+D entre grupos de investigacin de la Comunidad de Madrid en Tecnologias 2018. (Corresponding author: Miguel Sánchez.)

The authors are with the Department of Electronic Technology, University Carlos III de Madrid, Av de la Universidad, 30, 28911 Leganés, Madrid, Spain (e-mail: migusanc@ing.uc3m.es; dgallego@ing.uc3m.es; horacio@ing.uc3m.es).

Digital Object Identifier 10.1109/JPHOT.2021.3093863

to the solid state lasers. The main factor that limits the peak power in HPDLs is the effect known as catastrophic optical damage (COD) [17], a phenomenon by which the laser device is damaged and its emission power greatly decreases. Typically, the manufacturers only specify the maximum current of the HPDLs in normal operation conditions where pulse width is equal to 100 ns and the repetition rate is 1 kHz. These maximum current specifications are very conservative when the pulse durations are reduced from the normal operation. Consequently, it is possible the operation beyond the maximum current specification without damage.

In this work we have studied and compared the performance of four HPDLs that have been driven to generate up to 4 times the maximum rated output peak power by reducing the pulse width to the range of sub-10 nanosecond without producing COD using a custom designed current driver able to generate pulses of more than 100 A, improving the characteristics of HPDLs for their use in short pulse and high speed applications.

II. THEORETICAL MAXIMUM PEAK POWER: CATASTROPHIC OPTICAL DAMAGE (COD)

The catastrophic optical damage is an effect that produces the degradation of active region facets and cavity [18]. This causes a decrease in the total power emitted by the HPDL. COD is produced through different mechanisms, either for continuous wave (CW) operation or pulse wave (PW) operation. Generally, the optical power emitted by a diode laser operating in CW mode and high currents is saturated by the joule effect, which is caused by the injected current. As the current increases further, the heat generation in the device will continue to grow, until COD occurs. However, in PW operation at moderate repetition rates, the average current injected into the laser, in the mA range, is low enough to prevent the production of a relevant thermal effect. Since the efficiency of the laser is not greatly affected by the increase in temperature, the maximum optical power can be increased just below the COD. The relationship between the maximum optical power and the pulse width is well described by the ‘square root law’ discovered by Eliseev [19] and widely studied by other authors [20], [21], where the power required to have COD (PCOD) is proportional to $t^{0.5}$ (t : pulse width), that is, the radiant intensity necessary to cause COD increases when the pulse width decreases (Fig. 1). Following this, a HPDL can operate at higher currents compared to its nominal values to obtain a higher maximum optical power by reducing the current pulse duration. This maximum power is related to the maximum power density that the facets of the laser cavity can withstand without degradation. A rise in facet temperature occurs when the power density reaches a critical level, leading to its melting. This effect produces a recrystallization of the semiconductor material near the facet, increasing absorption and significantly reducing the power emitted. The value of this critical power density depends on various parameters of the laser, such as structure, facet design, construction materials, heat dissipation capacity, among others [20]. Generally, modern diode lasers with broad area, high-efficiency and high-reliability can withstand maximum power densities of around 20 MW/cm² in CW

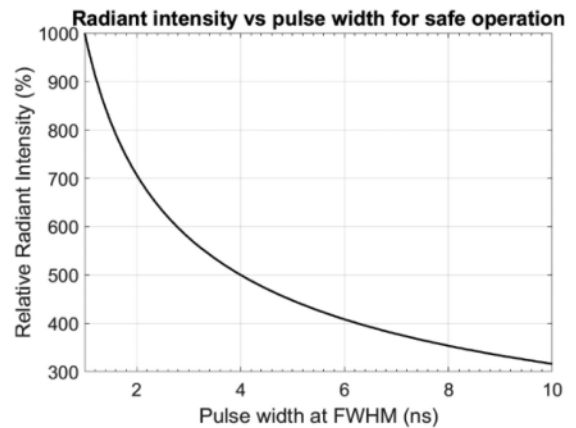


Fig. 1. Square-root law: with short pulses we can increase the nominal peak power without COD, the line determines the maximum relative radiant intensity and limit a safe region of operation based on peak power and pulse width.

TABLE I
HPDLs NOMINAL CHARACTERISTICS

Laser	Nominal peak power (W)	Pulse width ¹ (ns)	Current (A)	Emitting area (μm)	Packaging (Inductance)
TPGAU3S09H	225	100	30	225x340	U (5nH)
905D3J09S	200	100	35	235x400	S (5.2nH)
SPL PL90_3	75	100	30	200x10	Plastic (-)
TPGAD1S09H	70	100	30	229x10	SMT (1.6nH)

1. Full Width Half Maximum (FWHM)

operation [22] and around 30 MW/cm² in PW operation with pulse width of hundreds of nanoseconds [23], [24].

III. HIGH POWER DIODE LASERS UNDER STUDY

The capability to exceed the specified maximum optical power of four commercially available lasers have been tested: TPGAU3S09H (Excelitas Technologies Corp, Waltham, MA, USA), 905D3J09S (Laser Components GmbH, Olching, Germany), SPL PL90_3 (OSRAM Opto Semiconductors, Munich, Germany) and TPGAD1S09H (Excelitas Technologies Corp). The first two lasers are a stack of three chips. Each of those laser chips is formed by three emitter stripes (multi-junction). The third laser is a low-cost high-volume application device made up of a single chip with three emitter stripes (multi-junction). The last one is a surface-mount packaging laser with very low inductance composed of a single chip with three emitter stripes (multi-junction) as well. Table I summarizes their nominal characteristics specified by the manufacturers. A microscope image of the cavities of the lasers chips is shown in Fig. 2(a) and Fig. 2(b).

Fig. 3(a) and Fig. 3(b) show the maximum peak power and the expected maximum power density in the front facet for each laser under study as function of the pulse width according to their nominal maximum peak power and the square root law (Fig. 1), respectively. Since the stacked devices (TPGAU3S09H and 905D3J09S) are composed of three chips, correspondingly their

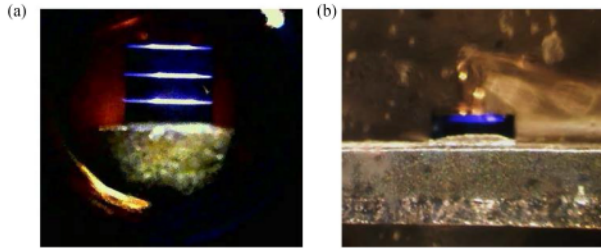


Fig. 2. (a) Near field emission of TPGAU3S09H, triple stack chip with 3 emitter stripes each chip. (b) Near field emission of SPL PL903, single chip with 3 emitter stripes.

maximum peak power is three-fold of the single chip devices (SPL PL90_3 and TPGAD1S09H). Regarding the optical power density, the four lasers have closer values, especially with larger current pulse widths. Small differences arise from the variations in the width of the cavity since the efficiency of these devices are similar. We use the maximum power density in CW mode (20 MW/cm^2) as value for the critical power density in order to ensure COD does not occur. This value determines that the minimum pulse width with the maximum peak power for these devices in safe operation is in the range between 5 ns and 10 ns (Fig. 3(b)) and it will be the objective operating regime.

IV. DRIVER DESIGN AND SIMULATIONS

In order to reach the maximum theoretical peak power, we need to supply the required current to the HPDL in pulses with duration lower than 10 ns, accordingly to Fig. 3(b). Consequently, to design a suitable current driver is necessary to consider the inductance of the circuit and to use very fast electronics. The two main elements that limit the pulse width and maximum peak current are the transistor driver and the power transistor. Currently, it is available in the market low side Gallium Nitride (GaN) drivers and enhancement mode GaN transistors (eGaN FET), that are much faster, cheaper, smaller and with better electrical characteristics than traditional silicon-based transistors [25]. The electrical schematic of proposed current driver is depicted in Fig. 4. A pulse shortener based on an AND gate and a RC low pass filter is activated by a square pulse generator. The GaN driver input pulse duration is given by the pulse width of V_{pulse} minus the fixed delay produced by the filter. The reduced width pulse activates the GaN driver that supplies enough current to activate the eGaN FET. While the pulse is not active a bank of capacitors is charged with a voltage source (V). When the eGaN FET is activated, stored energy is discharged through the HPDL generating a pulse of current. A clamping diode is positioned in parallel of the HPDL to protect of reverse overvoltage.

As we have described in Section III, we are going to test the capacity of four commercial lasers to achieve high peak powers without suffering COD. The Table II shows the maximum theoretical peak power and pulse width according to the Fig. 3(b) and the expected current needed to reach it for each HPDL. The higher current and the minimum pulse width of the Table II defines the requirements of our current driver.

TABLE II
HPDLs EXPECTED CHARACTERISTICS

Laser	Maximum expected peak power (W)	Pulse width ¹ (ns)	Expected Current (A)
TPGAU3S09H	810.8	7.7	103.6
905D3J09S	852.8	5.5	139.5
SPL PL90_3	240.8	9.7	105.9
TPGAD1S09H	276.8	6.4	113.8

1. FWHM

We have chosen the GaN driver LMG1020 (Texas Instruments, Dallas, TX, USA) with rise time less than 1 ns and the eGaN FET EPC2034 (Efficient Power Conversion, El Segundo, CA, USA) with maximum pulse current of 200 A. A bank of capacitors with a total of 104 nF supplies the energy of the pulses. The output of pulse shortener is a 5 ns pulse of 5 V amplitude and 1 kHz repetition rate. We have simulated the current generated with an ideal short-circuit and with an HPDL load model with series resistance of 0.2Ω and 5 nH inductance, typical values of commercial HPDLs. The simulations have been carried out with OrCAD 17.2 PSpice Designer software.

The first result of the simulation is the voltage necessary to reach the maximum current that will be demanded by HPDL at maximum expected peak power. Fig. 5(a) shows the characteristic curve of the driver with the HPDL load model, reaching a value of 144.9 A at a voltage of 120 V, fulfilling current requirements of the lasers under study. On the other hand, we need to check that the widths of the generated pulses are compatible with the calculated values. In Fig. 5(b) we present the shape of the pulses at 120 V with ideal short circuit and HPDL load model. In the ideal case of short circuit, we reach pulse currents up to 371.8 A, pulse width of 6.2 ns and rise and fall times of 1.7 ns and 0.7 ns, respectively. With the HPDL load model the series resistance and the inductance limit the current and the rise time obtaining a pulse width of 5.2 ns and a rise and fall time of 5.9 ns and 0.3 ns respectively, complying with the requirements indicated in the Table II as well.

These simulations verify that the topology of the circuit and the main components chosen for the construction of the current driver have sufficient capacity to generate the current pulses that will allow to test the HPDL outside their nominal operating regime, reaching much higher peak powers with pulses of reduced width.

V. EXPERIMENTAL MEASUREMENTS

The following experiments are intended to check the capability of the HPDLs to support high peak power without COD based on the theoretical limits discussed in Section III and to reach the peak power values indicated in the Table II. We have designed and built a current driver with capacity to generate ultra-short pulses with variable width and high current ($t < 10 \text{ ns}$ and $I > 100 \text{ A}$) with a rise time less than 3 ns. The current driver

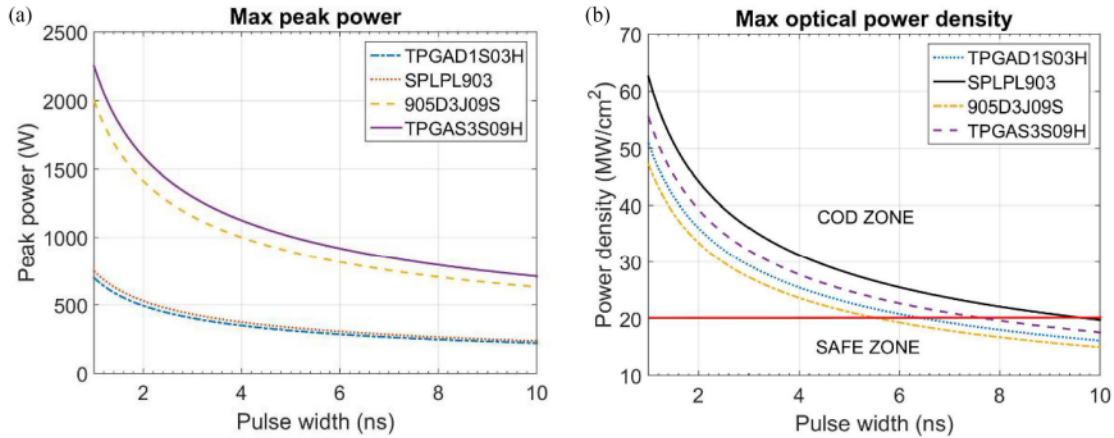


Fig. 3. (a) HPDLs maximum peak power based on the maximum ratings at the nominal pulse width for each laser and the square root law model. (b) Power density in the laser cavity versus optical pulse width. The solid red line represents the safe power density. The power density is a factor that limits the maximum peak power emitted by the laser cavity, since at higher values the laser facets will suffer COD.

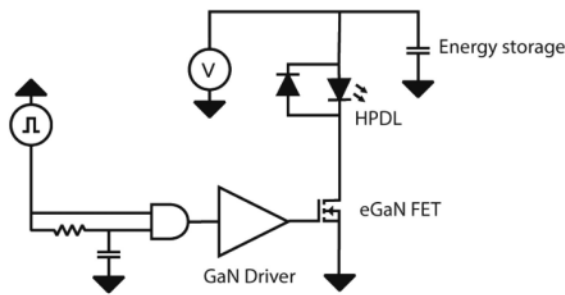


Fig. 4. Driver electrical schematic.

circuit has been designed considering the simulations indicated in Section IV. With short pulse durations and high currents, the effects of parasitic inductances (L_p) [26] can be very important, limiting the rise times of the pulses and the maximum current. We can reduce some of this L_p [27] taking special considerations in the design of the current driver such as the use of capacitors with low equivalent series resistance, minimizing ground return paths, clamping diodes to reduce the inductive overshoot due to the fast rise times of the current, split power loop to minimize the parasitic inductances and Kelvin gate to avoid ground lifting issues. Finally, the entire design has optimized tracks and via holes to reduce the inductance. The driver lacks a current monitor in order to not increase the current path inductance.

A. Characterization Setup

The Fig. 6 depicts the measurement setup to check the capability of the four proposed HPDLs to exceed their maximum rated optical peak power with high current short pulses. The pulse width and the repetition rate are controlled by an external pulse generator (HP 8112A, Keysight Technologies, Santa Rosa, CA, USA). The shape of the optical pulse is registered using a 1 GHz bandwidth avalanche photodiode module (APD C5658, Hamamatsu Photonics, Hamamatsu, Japan) connected to a 2 GHz oscilloscope (RTO1022, Rohde & Schwarz, Munich, Germany). The average power is measured using a calibrated

thermopile power meter (S401C Thorlabs, Newton, NJ, USA). An optical attenuator and a small aperture are placed between the laser and the APD detector, to avoid saturation of the detector by high peak power level and to avoid reflections that can widen the pulse, respectively. Finally, the captured temporal profile of the optical pulses is processed together with the average power and the repetition rate in order to obtain the peak power in real time. Each laser is tested following a procedure of several steps. First, the normal operation of the laser was checked, i.e., at nominal current, pulse width and duty cycle for correct operation assessment. From this starting point, the injected current, and therefore the peak power, were increased in steps while the current pulse width was decreased. During each step the pulse width and the optical peak power are monitored continuously for 60 seconds to check the stability. The optical peak power was raised and the pulse width decreased in steps until either the maximum optical density according to the discussion of Section III or the maximum driver voltage was reached.

B. Results

The tests of the four HPDLs were carried out using the setup and following the methodology indicated in the previous section. All the measurements have been done at 1 kHz repetition rate. Fig. 7 represents the temporal profile of the maximum optical peak power with the minimum pulse width duration for each laser. In the optical pulses we can see a secondary pulse after the main pulse due to resonance effects between the HPDL and the driver, even affecting the main pulse in the case of SPL PL90_3 (Fig. 7(c)). Besides this, there is pick-up noise produced by the high current pulses generated by the unshielded driver.

Table III shows the maximum peak power and the rest of the parameters obtained during the experiments without any noticeable damage. Higher peak powers at shorter pulses are possible to achieve, but the devices may suffer partial or total COD in a short operation time. The relative increase of the peak power respect to nominal value for each laser (Table III) is shown in the relative radiant intensity column.

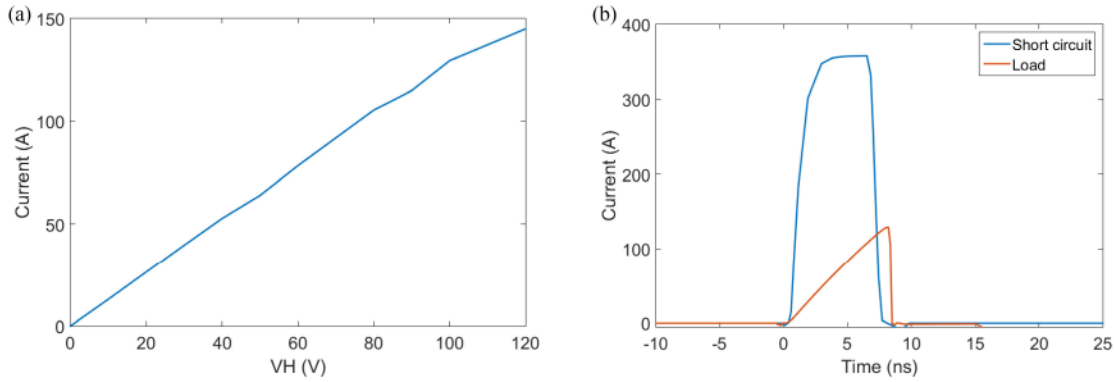


Fig. 5. (a) Peak power generated with HPDL load model (b) Current pulses with 120V with short circuit (6.2 ns FWHM and 371,8 A,) and HPDL load (5.2 ns FWHM and 144.9A).

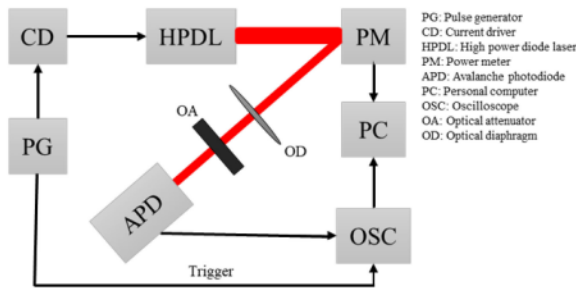


Fig. 6. Measurement block diagram.

TABLE III
HPDLs EXPERIMENTAL RESULTS WITHOUT COD

Laser	Maximum peak power (W)	Pulse width ¹ (ns)	Estimated current (A)	Power density (MW/cm ²)	Relative radiant intensity (%)
TPGAU3S09H	880.6	6	111.3	21.5	391
905D3J09S	697.1	5	119.8	16.5	348
SPL PL90_3	223.7	10	87.2	18.6	298
TPGAD1S09H	286.2	4	115.8	20.5	408

1. FWHM.

The higher optical power is achieved with TPGAU3S09H reaching a peak power of 880.6 W at 6 ns pulse width. The TPGAD1S09H with surface mount packaging shown the shortest pulse width and fastest rise time of all HPDL under test with 4 ns of pulse width, 2 ns rise time and reaching a peak power of 283.2 W. Comparing Tables II and III we can see that the currents obtained experimentally approach well the ones obtained in the simulations. The maximum current is 119.8 A at 110 V with the HPDL 905D3J09S being the maximum value expected of 135.5 A at 110 V.

The long-term stability while emitting the highest peak power has been studied for the SPL PL90_3 laser over a period of 22 hours with a pulse width of 10 ns and repetition rate of 1 kHz. The test room has an uncontrolled temperature around 23 °C and the HPDL does not have any type of cooling. Fig. 8 shows the variations in the output peak power during the measurements. In this experiment, 79.2 million pulses were emitted with an average peak power of 207 ± 2.6 W, which is almost 300% of

the nominal peak power of the laser. The fluctuations present in the graph are due to variations of the room temperature during the test and the use of a thermopile optical power detector which is sensitive to changes in temperature.

VI. DISCUSSION

Using our current driver, three of the lasers (TPGAU3SA9H, SPL PL90_3 and TPGAD1S09H) have their peak power limited by the safe power density that ensures that the facets do not suffer COD. In addition, the SPL PL90_3 suffers from a widened pulse profile when it is driven by high currents due to the resonance effects that occur between the laser and the current driver. In this case, a train of secondary current pulses were generated increasing the minimum width that can be achieved at high peak powers. This effect depends on the characteristics of the laser such as its operation voltage, inductance, series resistance and other parasitic factors.

On the other hand, the maximum optical peak power of the 905D3J09S laser is limited by the rise time of the current pulse at the maximum voltage that the current driver can withstand (110 V) due to the higher inductance of the packaging. When the current pulse width is increased, the current driver can supply the current required to reach the maximum power density of the laser. We show here the pulse width of 5 ns to demonstrate that very short pulses can be generated with this type of laser. Finally, note that the TPGAD1S09H laser has the shortest pulse width and fastest rise time among all tested lasers due to its low inductance surface mount packaging.

Typically, laser manufacturers are conservative with the nominal rates to ensure the high reliability of the device (around 15%), for example the HPDL SPL PL90_3 reports a maximum peak power with 100 ns pulse width of 90 W and the nominal value is 75 W.

The stability study shows that the laser SPL PL90_3 keeps the peak power level for a large amount of time demonstrating its reliability under these operating conditions. The peak power changes are principally caused by fluctuations in the thermopile offset due to room temperature changes during the experiment.

The proposed HPDLs sources offer significant improvement in the optical peak power and pulse width compared to

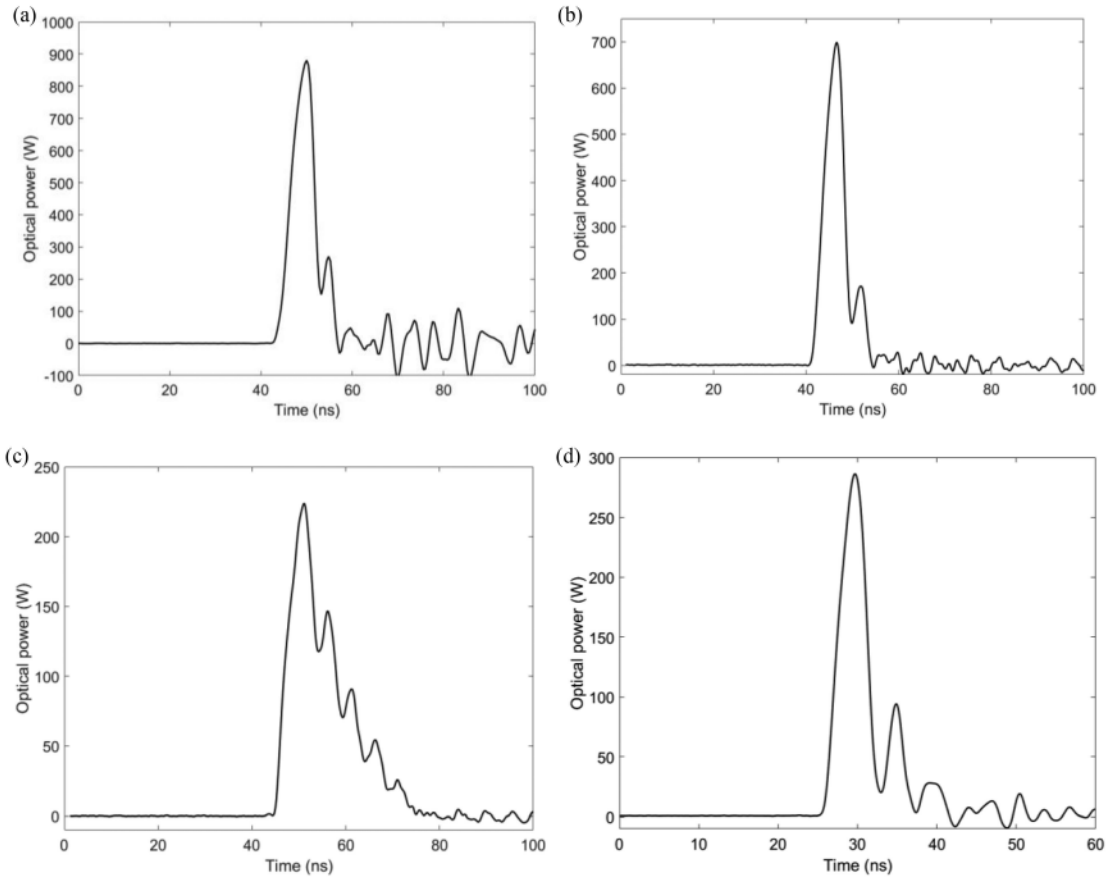


Fig. 7. Temporal profile of the optical peak power of the four lasers under study: (a) TPGAU3S09H, (b) 905D3J09S, (c) SPL PL90_3, (d) TPGAD1S09H.

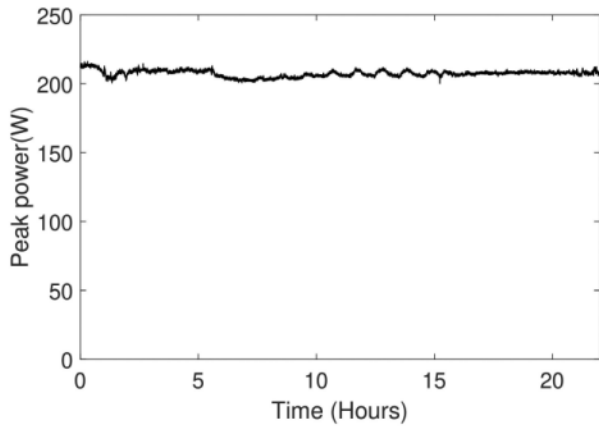


Fig. 8. Peak power stability of SPL PL90_3 during 22 hours emitting 10 ns pulses at a repetition rate of 1 kHz.

previously reported single laser diode-based systems. A report on optoacoustic microscopy [28] indicate a laser source with capacity to generate pulses up to 325 W and widths of 50 ns using a stacked single chip similar to lasers TPGAU3SA9H and 905D3J09S. Using our HPDLs, we will achieve an improvement in the optoacoustic efficiency conversion and in the resolution of the optoacoustic images. Regarding LIDAR sources, a laser system has been reported [29] with an optical peak power of

150 W and 200 ns pulse width. This system is more limited in measurement range and spatial resolution than one that used the lasers studied.

Finally mention that the traditional solution to overcome the lack of power of diode-based systems is the combination of multiple chips in bars and stacks. A laser array built by a stack of tens of bars, each with twenty TPGAU3S09H laser chips, can reach a maximum peak power of 174 kW and energies of 1 mJ in a pulse duration of 6 ns with a footprint of 32 mm². The main problem of this solution is the very poor beam quality of diode laser bars and stacks, which leads to the use of complex optics to correct the beam, although recently there were advances to solve this problem [30], [31]. Another simpler but less scalable solution is to combine multiple chips with a fiber package and individual current drivers [32]. With these peak powers and pulse widths this system would improve the performance of current multi-diode lasers (bars) optoacoustic systems imaging actually with peak powers of 10 kW, pulse duration of 136 ns and energies of 1.4 mJ [33] and could also improve the range of LIDAR systems by several orders of magnitude.

VII. CONCLUSION

In this work we have demonstrated for the first time to our knowledge the capacity of four different commercial lasers to generate high peak power pulses with a duration of few

nanoseconds beyond their maximum rating value given at their typical pulse width without causing COD. We have designed, simulated and built a custom high current short pulse driver based on new GaN transistors with a maximum current capacity of 120 A in a range of less than 10 nanoseconds pulse width and a repetition rate of 1 kHz to drive the HPDLs. With the commercial HPDL TPGAU3S09H we have achieved optical pulses with a maximum peak power of 880.6 W and 6 ns pulse width. This laser is rated to a maximum peak power of 225 W at 100 ns pulse duration. This corresponds to 391% of their maximum rated peak power. In addition, with the TPGAD1S09H laser we have reduced the pulse widths to only 4 ns and reach a peak power of 408% of its rated value. These noticeable increase in the peak power and reduce in the pulse width will mean improvements of range and resolution in applications such as LIDAR and optoacoustic biomedical techniques with respect to the conventional way to drive HPDLs.

REFERENCES

- [1] U. Andriolo, L. P. Almeida, and R. Almar, "Coupling terrestrial LiDAR and video imagery to perform 3D intertidal beach topography," *Coastal Eng.*, vol. 140, pp. 232–239, 2018.
- [2] D. S. Sawicki, *Traffic Radar Handbook: A Comprehensive Guide to Speed Measuring Systems*. Authorhouse, 2002.
- [3] D. Feng, L. Rosenbaum, F. Timm, and K. Dietmayer, "Leveraging heteroscedastic aleatoric uncertainties for robust real-time LiDAR 3D object detection," in *Proc. IEEE Intell. Veh. Symp. (IV)*, 2019, pp. 1280–1287.
- [4] M. Pierzchała, P. Giguère, and R. Astrup, "Mapping forests using an unmanned ground vehicle with 3D LiDAR and graph-SLAM," *Comput. Electron. Agriculture*, vol. 145, pp. 217–225, 2018.
- [5] M. E. Warren, "Automotive LiDAR technology," in *Proc. Symp. VLSI Circuits*, 2019, pp. C254–C255.
- [6] Y. Zhou, J. Yao, and L. Wang, "Tutorial on photoacoustic tomography," *J. Biomed. Opt.*, vol. 21, 2016, Art. no. 061007.
- [7] R. Esenaliev, "Optoacoustic diagnostic modality: From idea to clinical studies with highly compact laser diode-based systems," *J. Biomed. Opt.*, vol. 22, 2017, Art. no. 091512.
- [8] S. Jeon, J. Kim, D. Lee, J. W. Baik, and C. Kim, "Review on practical photoacoustic microscopy," *Photoacoustics*, vol. 15, 2019, Art. no. 100141.
- [9] M. Kneipp, J. Turner, H. Estrada, J. Rebling, S. Shoham, and D. Razansky, "Effects of the murine skull in optoacoustic brain microscopy," *J. Biophotonics*, vol. 9, pp. 117–123, 2016.
- [10] S. A. Ermilov *et al.*, "Three-dimensional optoacoustic and laser-induced ultrasound tomography system for preclinical research in mice: Design and phantom validation," *Ultrason. Imag.*, vol. 38, pp. 77–95, 2016.
- [11] W. Huang, W. Chang, J. Kim, S. Li, S. Huang, and X. Jiang, "A novel laser ultrasound transducer using candle soot carbon nanoparticles," *IEEE Trans. Nanotechnol.*, vol. 15, no. 3, pp. 395–401, May 2016.
- [12] P. K. Upputuri and M. Pramanik, "Dynamic in vivo imaging of small animal brain using pulsed laser diode-based photoacoustic tomography system," *J. Biomed. Opt.*, vol. 22, pp. 1–4, 2017.
- [13] T. Morita *et al.*, "Development of compact laser system with 1-J, 300-Hz by using high peak power laser-diode pumped Nd:YAG amplifiers for novel laser application," in *Solid State Lasers XXVIII: Technology and Devices*, edited by W. A. Clarkson and R. K. Shori, Ed., International Society for Optics and Photonics, SPIE, vol. 10896, pp. 87–93, 2019.
- [14] F. Bachmann, "Industrial applications of high power diode lasers in materials processing," in *Proc. Appl. Surf. Sci. 208-209, Phys. Chem. Adv. Laser Mater. Process.*, 2003, pp. 125–136.
- [15] J. Shemshad, S. M. Aminossadati, and M. S. Kizil, "A review of developments in near infrared methane detection based on tunable diode laser," *Sensors Actuators B: Chem.*, vol. 171–172, pp. 77–92, 2012.
- [16] A. Müller *et al.*, "Diode laser based light sources for biomedical applications," *Laser Photon. Rev.*, vol. 7, pp. 605–627, 2013.
- [17] H. Wenzel, P. Crump, A. Pietrzak, X. Wang, G. Erbert, and G. Tränkle, "Theoretical and experimental investigations of the limits to the maximum output power of laser diodes," *New J. Phys.*, vol. 12, 2010, Art. no. 085007.
- [18] M. Hempel *et al.*, "Microscopic origins of catastrophic optical damage in diode lasers," *IEEE J. Sel. Topics Quantum Electron.*, vol. 19, no. 4, pp. 1500508–1500508, Aug. 2013.
- [19] P. Eliseev, "Degradation of injection lasers," *J. Lumin.*, vol. 7, pp. 338–356, 1973.
- [20] F. Kappeler, K. Mettler, and K. Zschauer, "Pulsed-power performance and stability of 880 nm GaAlAs/GaAs oxide-stripe lasers," *IEE Proc. I - Solid-State Electron Devices*, vol. 129, pp. 256–261, 1982.
- [21] J. Tomm, M. Ziegler, M. Hempel, and T. Elsaesser, "Mechanisms and fast kinetics of the catastrophic optical damage (COD) in GaAs-based diode lasers," *Laser Photon. Rev.*, vol. 5, pp. 422–441, 2011.
- [22] I. B. Petrescu-Prahova *et al.*, "253 mW/ μm^2 maximum power density from 9xx nm epitaxial laser structures with Γ greater than $1\mu\text{m}$," in *Proc. IEEE 21st Int. Semicond. Laser Conf.*, 2008, pp. 135–136.
- [23] X. Wang *et al.*, "Root-cause analysis of peak power saturation in pulse-pumped 1100 nm broad area single emitter diode lasers," *IEEE J. Quantum Electron.*, vol. 46, no. 5, pp. 658–665, May 2010.
- [24] M. Hempel, J. Tomm, M. Ziegler, T. Elsaesser, N. Michel, M. Krakowski, "Catastrophic optical damage at front and rear facets of diode lasers," *Appl. Phys. Lett.*, vol. 97, no. 7, pp. 231101–231101, 2010.
- [25] A. Lidow, J. Strydom, M. D. Rooij, A. Ferencz, and R. White, "Driving eGaN FETs in high performance power conversion systems," *ECS Trans.*, vol. 41, pp. 113–125, 2019.
- [26] Z. Chen, D. Boroyevich, and R. Burgos, "Experimental parametric study of the parasitic inductance influence on mosfet switching characteristics," in *Proc. 2010 Int. Power Electron. Conf. - ECCE ASIA*, 2010, pp. 164–169.
- [27] J. Nissinen and J. Kostamovaara, "A 4 A peak current and 2 ns pulse width cmos laser diode driver for high measurement rate applications," in *Proc. ESSCIRC*, 2013, pp. 355–358.
- [28] M. Erfanzadeh, P. D. Kumavor, and Q. Zhu, "Laser scanning laser diode photoacoustic microscopy system," *Photoacoustics*, vol. 9, pp. 1–9, 2018.
- [29] Y. Qiu *et al.*, "Ultra-high-power and high-efficiency 905nm pulsed laser for LiDAR," in *Proc. IEEE 4th Optoelectron. Global Conf.*, 2019, pp. 32–35.
- [30] G. Lin, P. Zhao, Z. Dong, X. Lin, "Beam-shaping technique for fiber-coupled diode laser system by homogenizing the beam quality of two laser diode stacks," *Opt. Laser Technol.*, vol. no. 123, 2020.
- [31] M. Sánchez *et al.*, "Beam profile improvement of a high-power diode laser stack for optoacoustic applications," *Int. J. Thermophys.*, vol. 38, 2017, Art. no. 48.
- [32] L. Leggio *et al.*, "Multi-wavelength photoacoustic system based on high-power diode laser bars," in *International Society for Optics and Photonics*, SPIE, Bellingham, WA, pp. 591–604, 2017.
- [33] P. K. Upputuri and M. Pramanik, "Fast photoacoustic imaging systems using pulsed laser diodes: A review," *Biomed. Eng. Lett.*, vol. 8, pp. 167–181, 2018.